Geomechanics and Engineering, *Vol. 15, No. 4 (2018) 973-986*
DOI: https://doi.org/10.12989/gae.2018.15.4.973

Parametric study of the convergence of deep tunnels with long term effects: Abacuses

Felipe P. M. Quevedo* and Denise Bernaud[a]

Department of Civil Engineering Federal University of Rio Grande do Sul, 99 Osvaldo Aranha, Porto Alegre, Rio Grande do Sul, Brazil

(Received July 27, 2017, Revised December 20, 2017, Accepted January 6, 2018)

Abstract. The objective of this paper is to present abacuses obtained from a parametric study of deep-lined tunnels using a numerical finite element model. This numerical model was implemented in software GEOMEC91, which is a two-dimensional axisymmetric model that considers the progress of excavation and the placing of the lining through the activation and deactivation of elements. It is adopted a step of excavation constant (1/3 of radius), constant velocity and circular cross section along the tunnel axis. It is used for rock mass a viscoplastic constitutive law with von-Mises criterion of viscoplasticity without hardening whose deformation rate over time is given by the Bingham model. The lining uses a linear elastic constitutive law. In total are 1716 analysis presented in 60 abacuses that show the value of ultimate convergence (U_{eq}) due to tunneling speed. In addition, it is shown an example of the use of the abacuses to determine the ultimate convergence (U_{eq}) of the tunnel and pressure (P_{eq}) on the lining.

Keywords: tunnels; finite element method; long-term analysis; elastic lining; soil-structure interaction

1. Introduction

Stabilizing underground openings such as tunnels excavated in rock mass remain a major concern of geotechnical engineers dealing with this kind of structures. In tunnels, the rock mass strain and the ground pressure on lining depend on the stress state and characteristics of the rock mass as well as of the geometry, the stiffness and the moment of the lining installation. Pressure variation on lining and strain over time are caused by the advance of excavation and the time-dependent properties of the rock mass and lining.

For a long time, these engineering works were designed based on the experience of the engineers, the similarity to “reference works” and empirical methods. Nowadays, the computational tools allow the study of tunnels with three-dimensional models that consider the nonlinearity of the materials and the ground-support interaction together with the constructive process. Works such as the Mroueh & Shahrour (2003), Gomes (2006), Masin (2009), Couto (2011), Machado (2011) and Fiore (2015), exemplify some of these tools. In the case of viscoplastic behavior of the rock mass, several other studies consider the long-term effects. We can mention some studies such as Hanafy (1981), Sulem *et al.* (1987), Bernaud (1991), Pan and Dong (1991a, b), Bernaud *et al.* (1994), Benamar (1996), Malan (1999), Sahli *et al.* (2001), Boidy & Pellet (2002), Gomes (2006), Sterpi and Gioda (2009), Debernardi (2008), Debernardi & Barla (2009) and more recently, Fahimifar *et al.* (2010), Roatesi (2010), Barla *et al.* (2011), Nomikos, *et al.* (2011), Khoshboresh (2013), Karami and Fahimifar (2013), Sharifzadeh *et al.* (2013), Wang *et al.* (2013, 2014), Maleki and Mousivand (2014), Fiori *et al.* (2016) and Quevedo (2017).

However, these analyzes require meshes that are difficult to construct and have longer processing time and, therefore, reserved for more complex studies (which consider rock mass heterogeneity, localized loading of surface structures, noncircular sections, partial excavations, etc.). Beyond that, the tunneling project involves step-decision where the designer does not have much information and needs to do quick preliminary studies. Tools that allow quick and cost-effective evaluation may be helpful in these steps. Therefore, the scope of this work is to present the results of a parametric study with an axisymmetric two-dimensional model of a tunnel excavated in a rock mass with viscoplastic behavior and elastic lining. The numerical simulation of the tunnel advance is based on the technique of activating and deactivating elements. The following parameters are changing in the calculation:

- the distance of the lining to the excavation face;
- the modulus of elasticity of the rock mass;
- the stiffness of the lining;
- the hydrostatic geostatic pressure;
- the excavation speed.

2. Numerical model

Tunnels are essentially three-dimensional problems. However, for long stretches and sufficiently deep tunnels (depth/radios of cross-section $\geq$ 10) within sufficiently homogeneous ground/rock mass, axisymmetric conditions

*Corresponding author, M.E.
E-mail: motta.quevedo@ufrgs.br
[a]Ph.D.
E-mail: denise.bernaud@ufrgs.br

http://www.techno-press.org/?journal=gae&subpage=7
ISSN: 2005-307X (Print), 2092-6219 (Online)

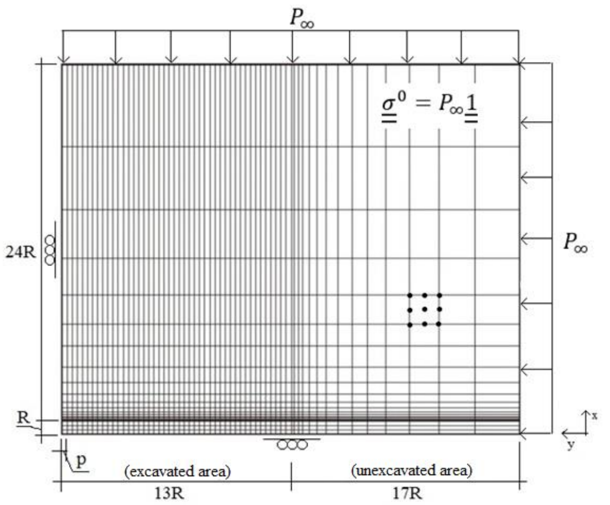

Fig. 1 Finite element mesh and boundary conditions of the model (Bernaud 1991)

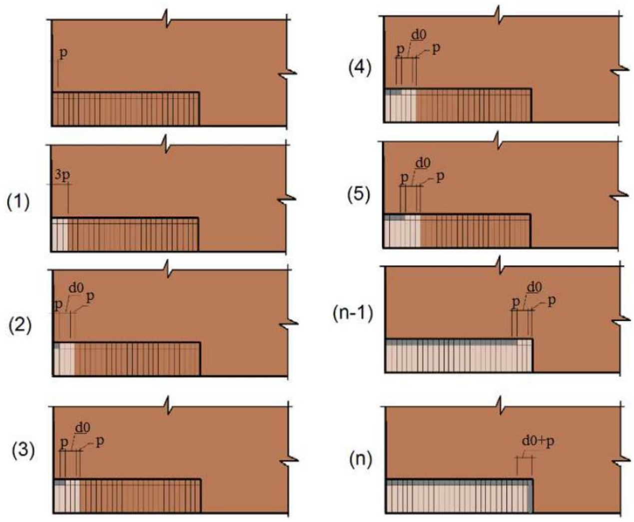

Fig. 2 Sequence of excavation and placement of the lining (QUEVEDO 2017)

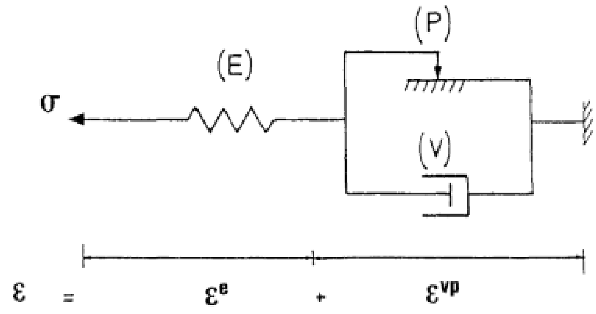

Fig. 3 Sequence of excavation and placement of the lining (Bernaud 1991)

around the longitudinal axis of the tunnel may be considered valid. These considerations allow simplifying the rigorously three-dimensional problem for a two-dimensional axisymmetric analysis. However, this simplification restricts the study to circular sections and deep-long tunnels. Despite the limitations of the model, these simplifications allow larger amounts of analysis since it is a less costly model from the computational point of view.

2.1 Numerical simulation procedure

The model used in the calculations can be seen in Fig. 1. A regular mesh composed of 1298 quadrilateral, isoparametric elements with nine nodes and quadratic interpolation functions was used. The model has dimensions of 24R along the x axis and 30R along the y axis (longitudinal axis of the tunnel). The excavated portion corresponds to a length of 13R around the tunnel axis, where R is the radius of the circular section of the tunnel.

To represent the excavation, at each step of excavation, a low multiplier is applied in the modulus of elasticity of the corresponding elements deactivating them. The velocity of the excavation V was considered constant and simulated through the time required to excavate a single step, according to Eq. (1)

$$t_p = p/V \tag{1}$$

where t_p = time required to a step of the excavation, p = excavation step, V = excavation speed. The placement of the lining along the excavation was simulated by changing the properties of the finite elements to the elastic properties of the lining. Fig. 2 illustrates the tunneling process, the first excavation consisting of three steps (3p=R) and the remainder step-by-step excavation, in 36 excavations. The installation of the lining follows the excavation distance d_0 (unsupported length) from excavation face.

After the excavations, the lining corresponding to the last excavation is filled. Afterwards, the program continues simulating the behavior of the tunnel over time until the increase in viscous deformation is below a certain tolerance, thus achieving stabilization of the deformations and of the tensions of the tunnel.

2.2 Constitutive laws

The constitutive law of the viscoplastic rock mass is represented according to the rheological diagram presented in Fig. 3.

The tensor of total deformations was decomposed according to Eq. (2)

$$\underline{\underline{\varepsilon}} = \underline{\underline{\varepsilon}}^e + \underline{\underline{\varepsilon}}^{vp} \tag{2}$$

where $\underline{\underline{\varepsilon}}^e$ e $\underline{\underline{\varepsilon}}^{vp}$ are the elastic and viscoplastic strain tensors, respectively. The total stress $\underline{\underline{\sigma}}$ was obtained by Hooke's law, according to Eq. (3)

$$\underline{\underline{\sigma}} = \underline{\underline{\underline{\underline{D}}}} : \left(\underline{\underline{\varepsilon}}^e - \underline{\underline{\varepsilon}}^{vp}\right) + \underline{\underline{\sigma}}^0 \tag{3}$$

where $\underline{\underline{\underline{\underline{D}}}}$ is the 4th order tensor with the elastic properties of the ground and $\underline{\underline{\sigma}}^0$ is the initial stresses. To determinate if the stress state is in an elastic or viscoplastic regime, the

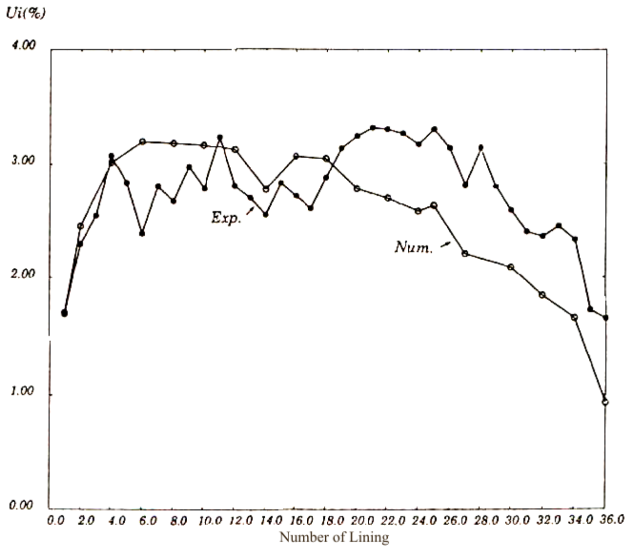

Fig. 4 Comparison of experimental and numerical convergence for t = 4 years (Bernaud and Rousset 1993)

von-Mises viscoplasticity criterion represented by Eq. (4) was adopted

$$F(\underline{\underline{\sigma}}) = \sqrt{\frac{3}{2}}\left\|\underline{\underline{\sigma}}^D\right\| - \sigma_s \tag{4}$$

where $\left\|\underline{\underline{\sigma}}^D\right\|$ is the modulus of the deviatoric stresses and σ_s is the yield stress obtained by a test, which in the case of geomechanical materials is equal to 2 times the cohesion. When $F(\underline{\underline{\sigma}}) \le 0$ the tensile state in elastic domain and the total strain rate is purely elastic, according to Eq. (5)

$$\dot{\underline{\underline{\varepsilon}}} = \dot{\underline{\underline{\varepsilon}}}^e \tag{5}$$

However, if $F(\underline{\underline{\sigma}}) \le 0$ the total strain rate is the sum of an elastic part and a viscoplastic part, according to Eq. (6)

$$\dot{\underline{\underline{\varepsilon}}} = \dot{\underline{\underline{\varepsilon}}}^e + \dot{\underline{\underline{\varepsilon}}}^{vp} \tag{6}$$

The Bingham model was adopted for the viscoplastic deformation rate, according to Eq. (7)

$$\dot{\underline{\underline{\varepsilon}}}^{vp} = \frac{1}{\eta}\left\langle \frac{F(\underline{\underline{\sigma}})}{F_0} \right\rangle^n \frac{\partial G(\underline{\underline{\sigma}})}{\partial \underline{\underline{\sigma}}} \tag{7}$$

where $F(\underline{\underline{\sigma}})$ is the viscoplasticity criterion, $G(\underline{\underline{\sigma}}) = F(\underline{\underline{\sigma}})$ is the associated viscoplastic potential, η and n=1 are viscosity constants, F_0 represents a reference tension and ⟨·⟩ is the Macaulay brackets. For the lining adopted the Hooke's law according to Eq. (8)

$$\underline{\underline{\sigma}} = \underline{\underline{\underline{D}}} : \underline{\underline{\varepsilon}}^e \tag{8}$$

where $\underline{\underline{\underline{D}}}$, in this case, is the 4th order tensor with the elastic properties of the lining.

2.3 Verification and validation of GEOMEC91

The model used in this paper is implemented in the finite element code GEOMEC91 which was largely verified with analytical solutions (perfect and hardening plastic Tresca, Coulomb, von-Mises and Drucker-Prager constitutive laws) (Bernaud 1991) and validated with the experimental results of a deep viscoplastic clay in the gallery of Mol in Belgium (Bernaud and Rousset 1993). In this case of the Mol's gallery, considering velocity of the excavation variable, elastic nonlinear linning and a hardening parameter in the viscoplasticity criterion, the code showed its efficacy in a more complex problem than the present work, reaching a good approximation of the real long term convergences, as shown in Fig. 4.

3. Numerical model

According to Bernaud (1991), eight parameters can be used to analyze the problem in perfect viscoplasticity: P_∞ hydrostatic geostatic pressure, K_s stiffness of the lining, d_0 unsupported length, V tunneling speed, η mass viscosity coefficient, R radius of cross-section of the tunnel and C the cohesion of the rockmass. These parameters can be grouped into five independent dimensionless parameters, according to Eqs. (9)-(13).

$$\mathrm{E}_s^* = \frac{E_s}{C} \tag{9}$$

$$\mathrm{P}^* = \frac{P_\infty}{C} = \frac{\gamma H}{C} \tag{10}$$

$$\mathrm{K}_s^* = \frac{K_s}{C} \tag{11}$$

$$\mathrm{d}_0^* = \frac{d_0}{R} \tag{12}$$

$$\mathrm{V}^* = \frac{V\eta}{CR} \tag{13}$$

where γ is the specific weight to the ground/rock mass, H the depth of the tunnel and K_s is obtained through the equivalent rigidity of a thick circular tube (radius/thickness ≤10) according to Eq. (14) (Panet 1995).

$$\mathrm{K}_s = \frac{E_r(R^2 - (R-e)^2)}{(1+\upsilon_r)\left[(1-2\upsilon_r)R^2 + (R-e)^2\right]} \tag{14}$$

where E_r is the modulus of elasticity of the lining, ν_r is the Poisson's coefficient of the lining, e is the thickness of the lining and R is the radius of the cross-section of the tunnel. Each analysis performed generates a convergence profile as shown in Fig. 5. The convergence in equilibrium U_{eq} corresponds to the mean of the convergences U in a stretch between 23R and 26R after cessation of viscous effects.

The convergence profiles will not be presented, only the abacuses that collect the U_{eq} results as a function of the

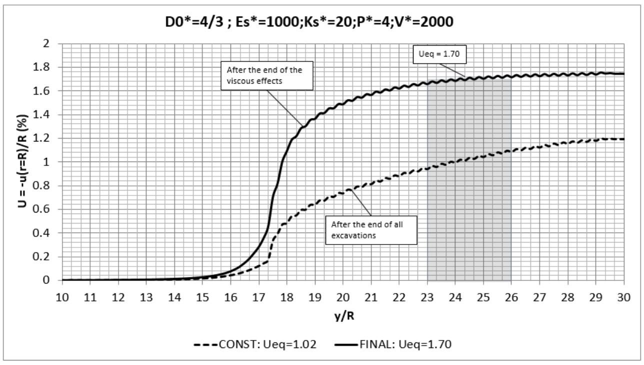

Fig. 5 Example of convergence profile

Table 1 Values of the dimensionless parameters used to construct the abacuses

Dimensionless parameters (Group 1)						
d0*	0,00	0.67	1.33			
Es*	80	400	1000	1600	3200	
Ks*	20	200	400	800	2000	
P*	2	4				
v*	100	250	580	800	1160	2000
Dimensionless parameters (Group 2)						
d0*	0.00	0.67	1.33			
Es*	333	1667	41667	6667	13333	
Ks*	83	833	1667	3333	8333	
P*	8	17				
v*	100	250	580	800	1160	2000

unlined distance d_0*, the velocity of tunneling V* and the equivalent stiffness of the lining K_s*. The Poisson's coefficient adopted for the rock mass was ν_s.= 0.4 and the dimensionless parameters used in the analysis are show in Table 1.

Another important parameter for preliminary analyzes is the equilibrium pressure P_{eq} acting on the lining. For a Tresca rock mass, we can obtain the convergence curve given by the analytical solution presented in Eqs. (15)-(17) for R = 1 (Bernaud 1991)

$$y = \exp\left(\frac{P_\infty - P_i}{2C} - \frac{1}{2}\right) \tag{15}$$

$$P_{\lim} = P_\infty - C \tag{16}$$

$$U_i = \begin{cases} \dfrac{1+\nu_s}{E_s}(P_\infty - P_i) \leftrightarrow P_i \geq P_{\lim} \\ \dfrac{1+\upsilon_s}{E_s}\left[2C(1-\upsilon_s)(y)^2 - (1-2\upsilon_s)(P_\infty - P_i)\right] \leftrightarrow P_i \leq P_{\lim} \end{cases} \tag{17}$$

Since Eq. (17) is deduced considering Tresca's Plasticity criterion, the C cohesion makes the approach between the Tresca and von-Mises models. It's given by Eq. (18)

$$C_{VM} = \frac{2}{\sqrt{3}} C_{TR} \tag{18}$$

Adopting as an approximation ν_s.= 0.5 we have an explicit form to calculate P_{eq}, according to Eq. (19) (Bernaud and Rousset 1992)

$$P_{eq} = P_\infty - C_{VM}\left[1 + \ln\left(\frac{2U_{eq}E_s}{3C_{VM}}\right)\right] \tag{19}$$

4. Results

The results of the study are summarized in the abacuses of Figs. 6-21. These abacuses can be used for preliminary studies; however, convergences greater than 20% are unrealistic and are useful only for academic studies.

Through the abacuses it is possible to see the influence of some parameters on the final convergence of the tunnel excavated in rock mass with viscoplastic effects:

• the greater the unlined distance, the greater the radial deformation;

• the higher the speed, the smaller the radial deformation. However, for P* values less than 2, velocity does not influence radial deformation;

• for P* greater than 2, the slower the speed, the greater the sensitivity of the convergence;

• the greater the stiffness of the lining, the smaller the radial deformation. However, the approximation of the curves for high stiffness indicates a limit from which the increase in stiffness no longer influences the convergence;

• It can be observed in most cases that the curves for different stiffness are parallel.

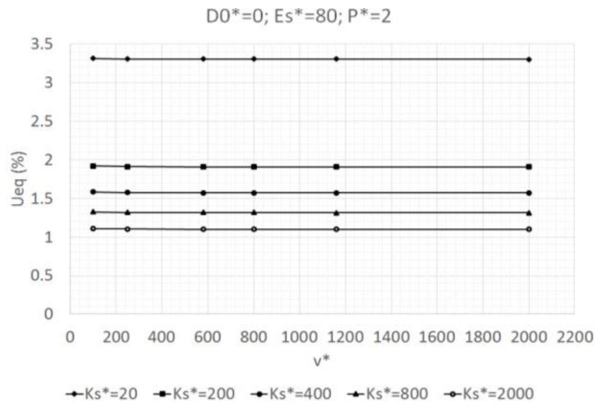

(a)

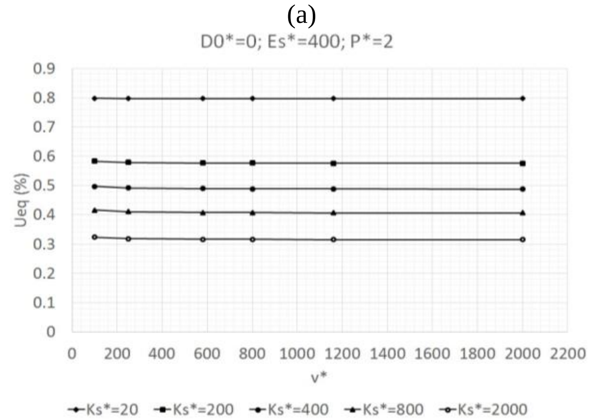

(b)

Fig. 6 Group 1: D0*=0, P*=2, Es*=80 to 1600

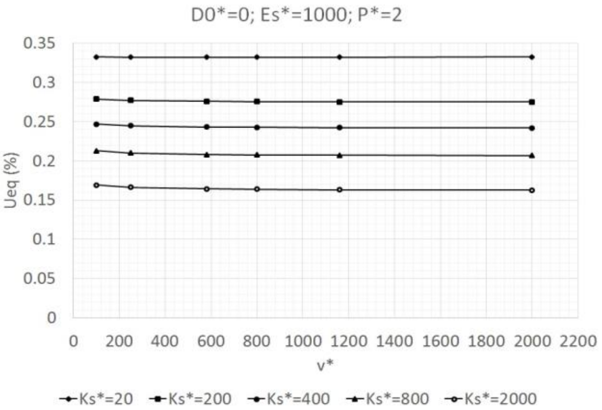

(c)

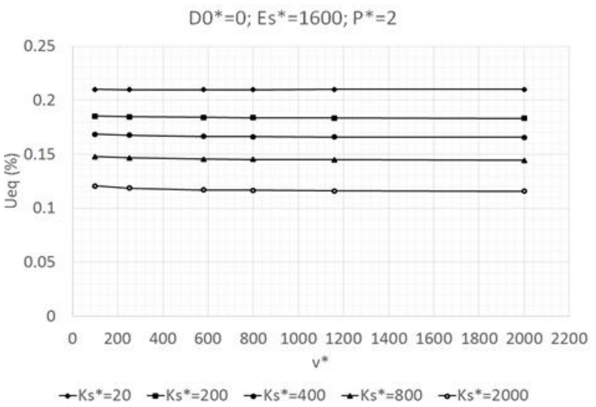

(d)

Fig. 6 Continued

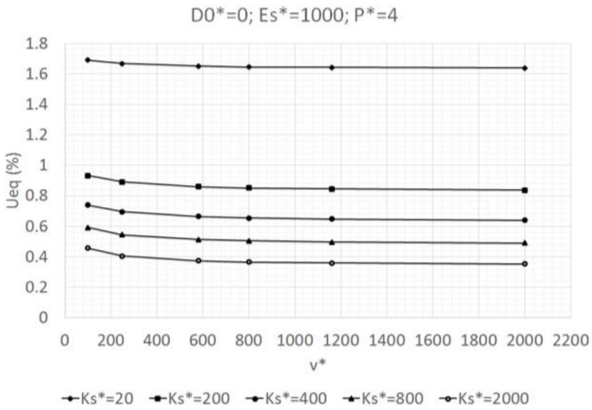

(c)

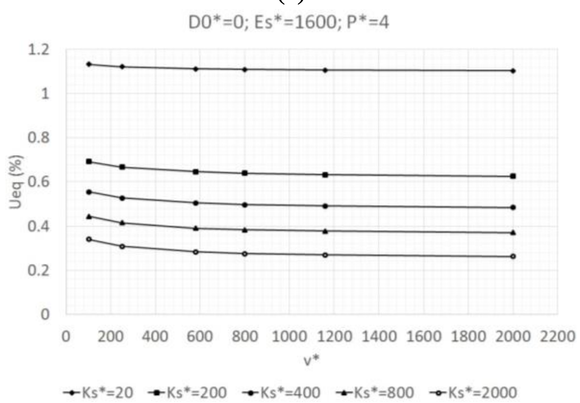

(d)

Fig. 7 Continued

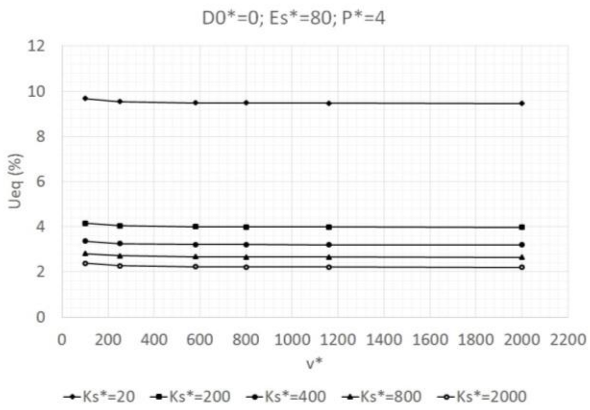

(a)

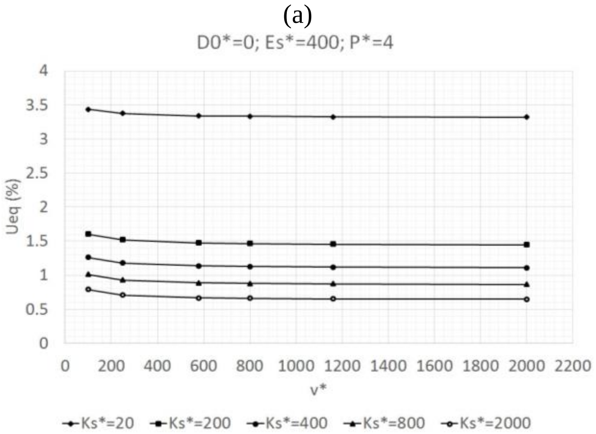

(b)

Fig. 7 Group 1: D0*=0, P*=4, Es*=80 to 1600

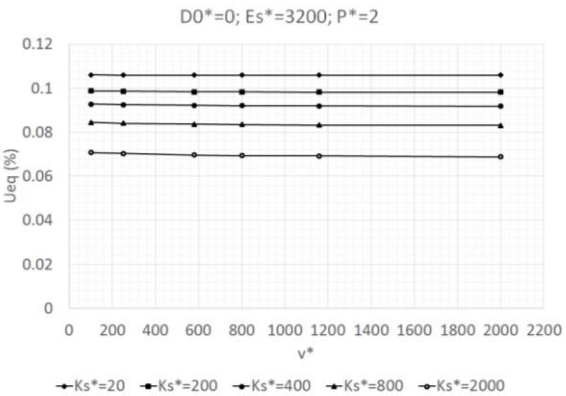

(a)

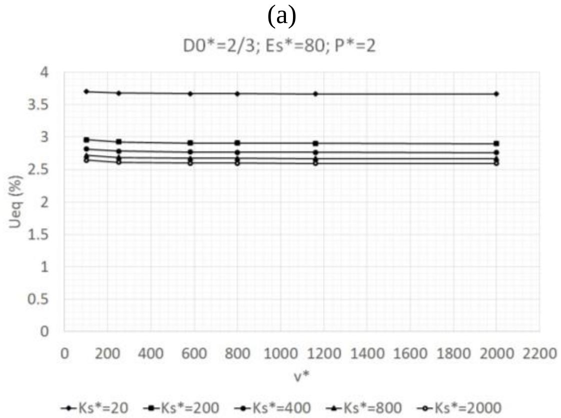

(b)

Fig. 8 Group 1: D0*=0, P*=2, Es*=3200; D0*=2/3, P*=2 Es*=80 to 1000

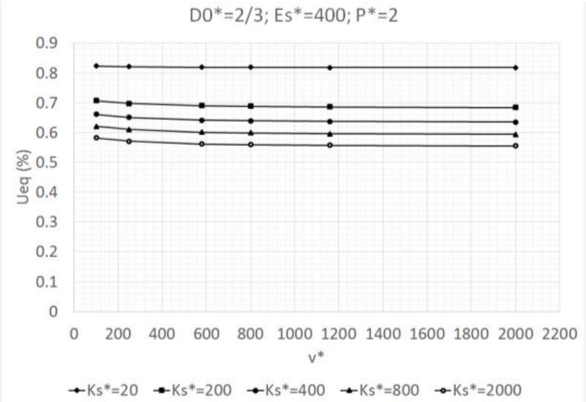

(c)

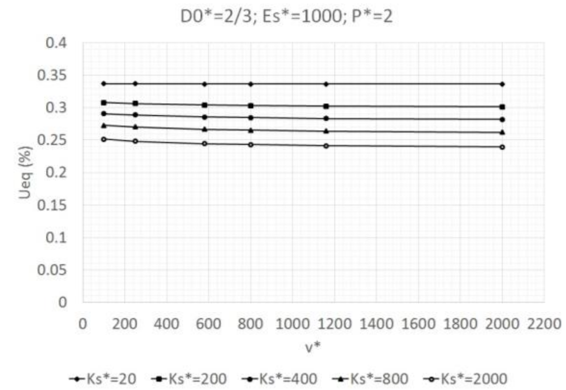

(d)

Fig. 8 Continued

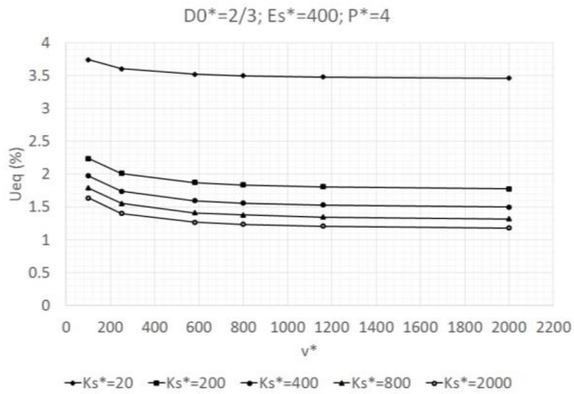

(c)

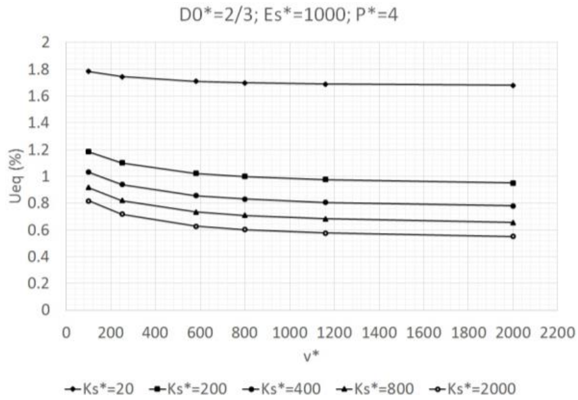

(d)

Fig. 9 Continued

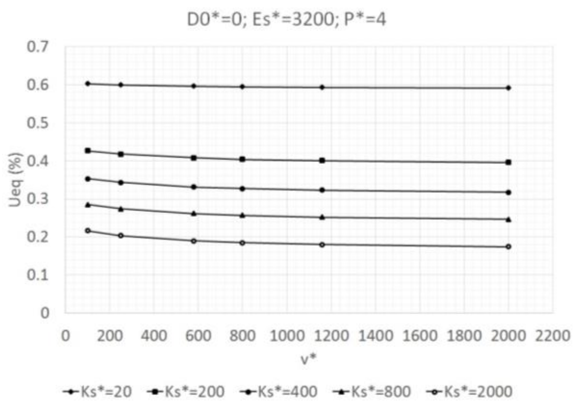

(a)

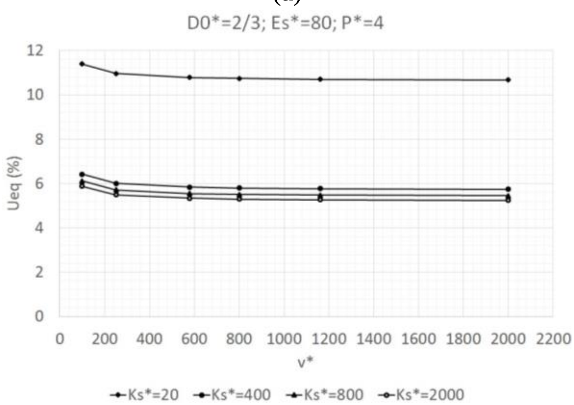

(b)

Fig. 9 Group 1: D0*=0, P*=4, Es*=3200; D0*=2/3, P*=4 Es*=80 to 1000

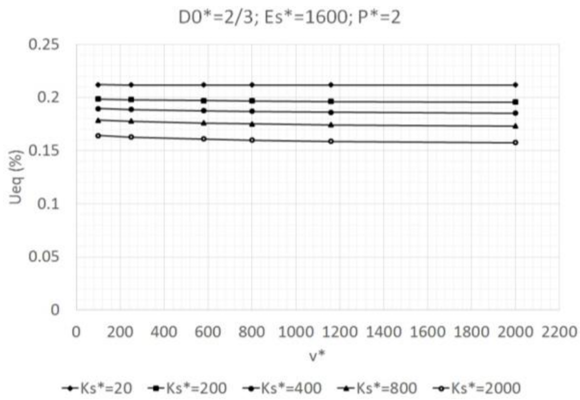

(a)

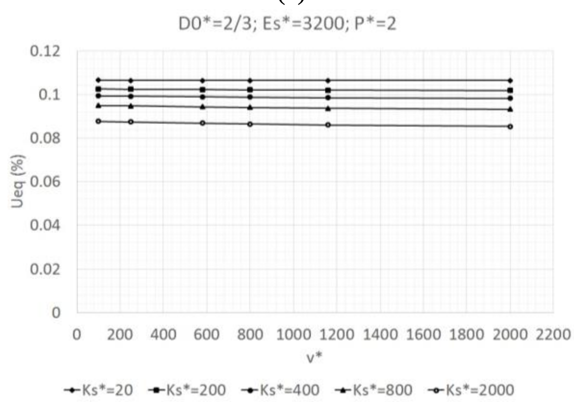

(b)

Fig. 10 Group 1: D0*=2/3, P*=2 Es*=1600 to 3200; D0*=4/3, P*=2 Es*=80 to 400

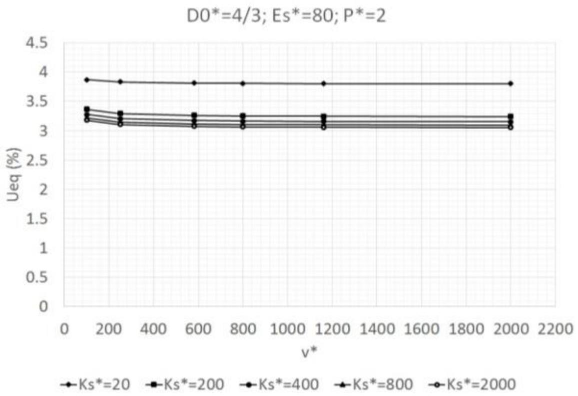

(c)

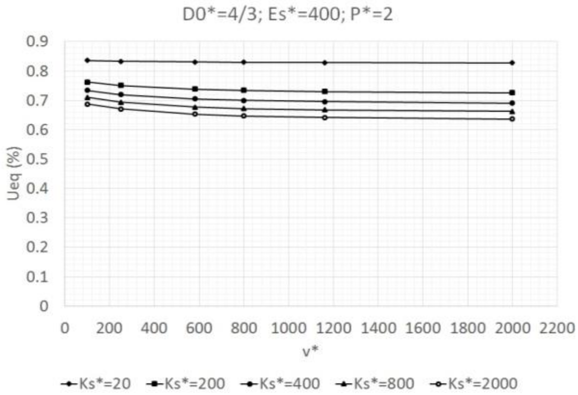

(d)

Fig. 10 Continued

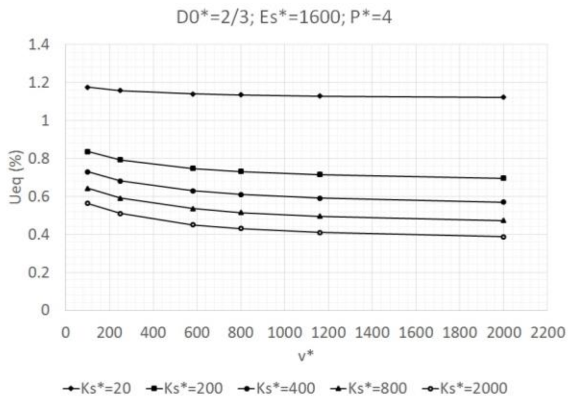

(a)

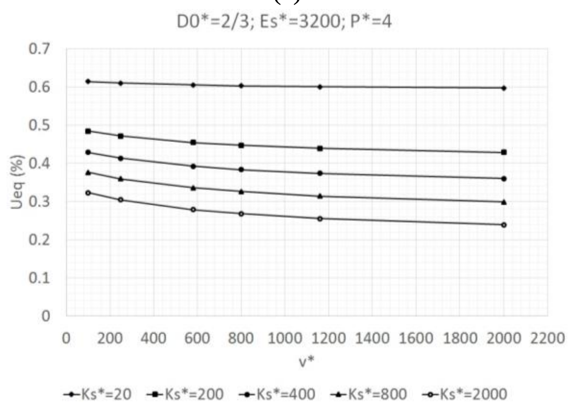

(b)

Fig. 11 Group 1: D0*=2/3, P*=4, Es*=1600 to 3200; D0*=4/3, P*=4, Es*=80 to 400

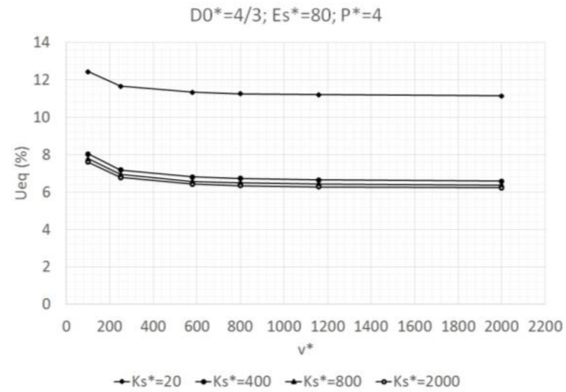

(c)

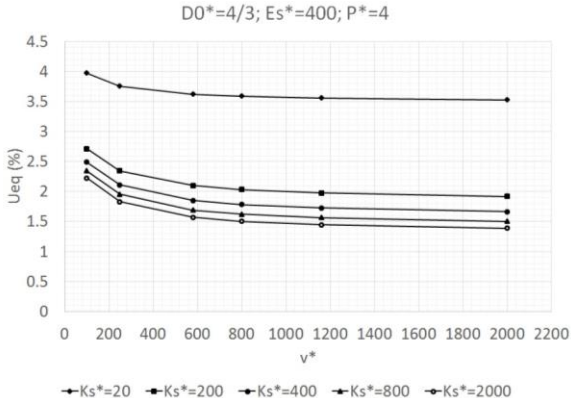

(d)

Fig. 11 Continued

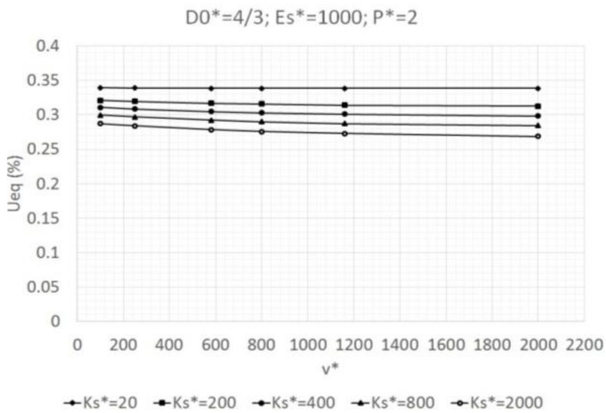

(a)

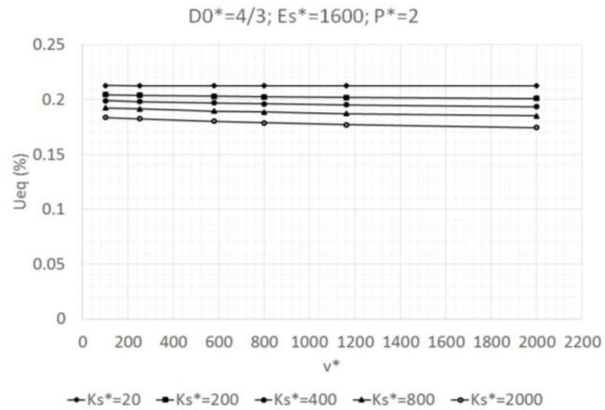

(b)

Fig. 12 Group 1: D0*=4/3, P*=2, Es*=1000 to 3200

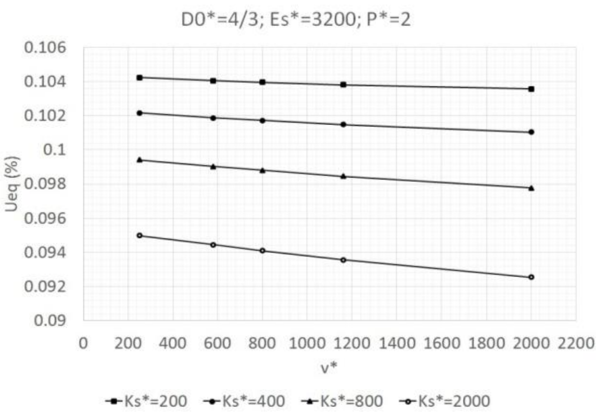

(c)

Fig. 12 Continued

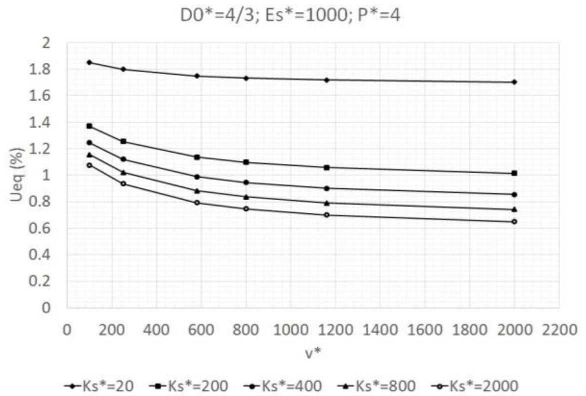

(a)

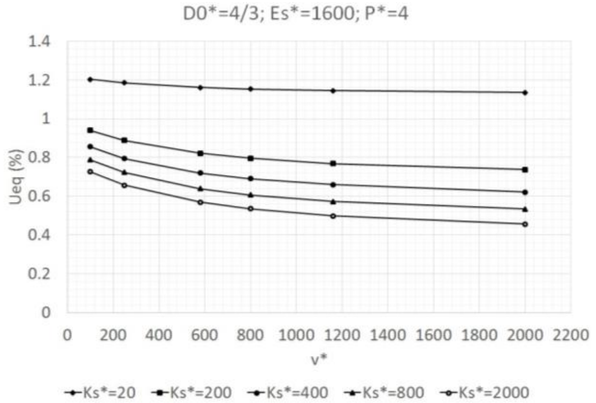

(b)

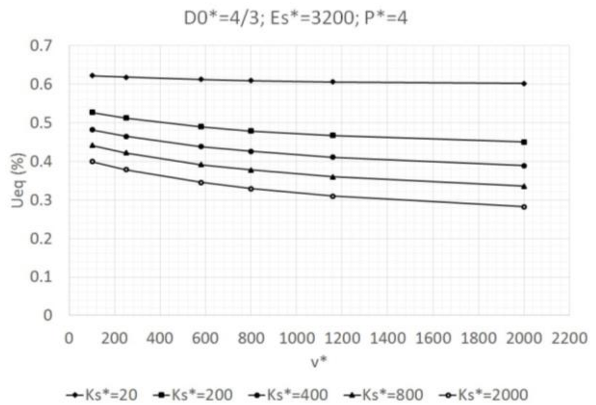

(c)

Fig. 13 Group 1: D0*=4/3, P*=4, Es*=1000 to 3200

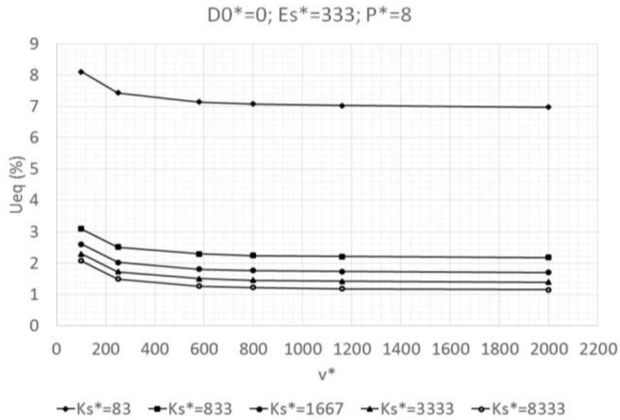

(a)

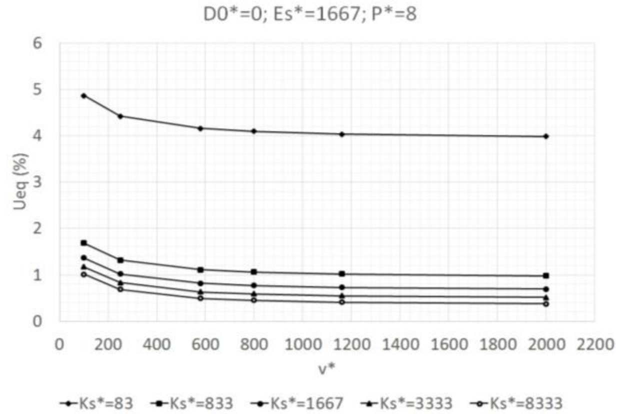

(b)

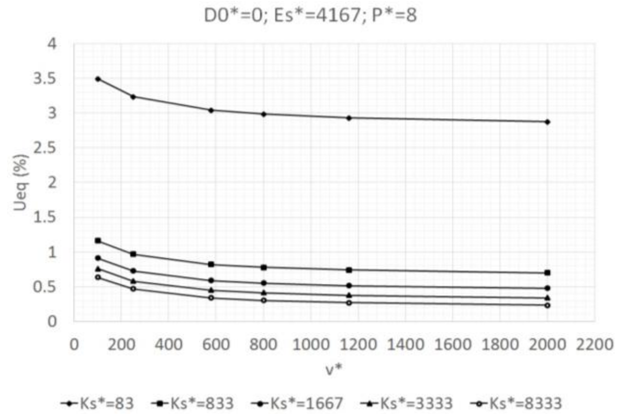

(c)

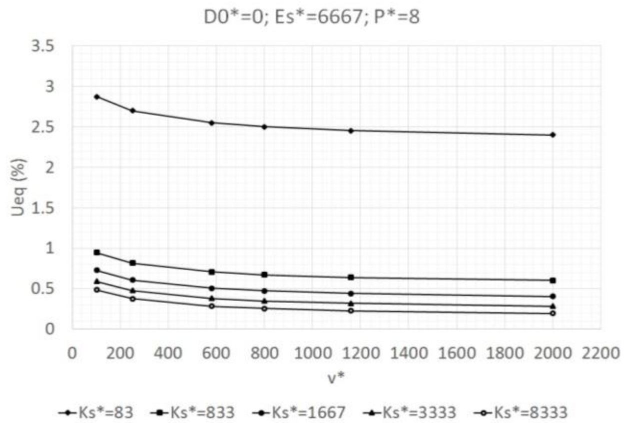

(d)

Fig. 14 Group 2: D0*=0, P*=8, Es*=80 to 6667

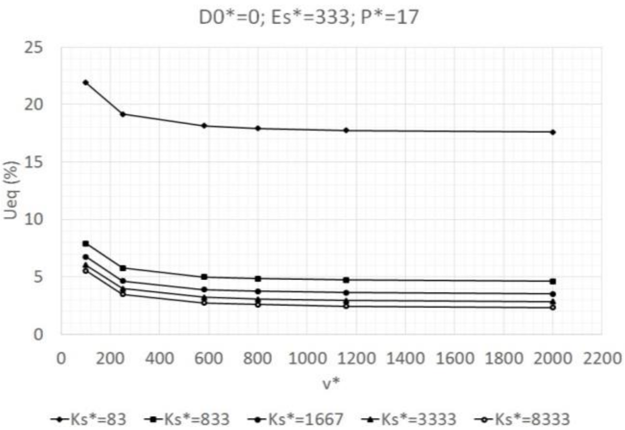

(a)

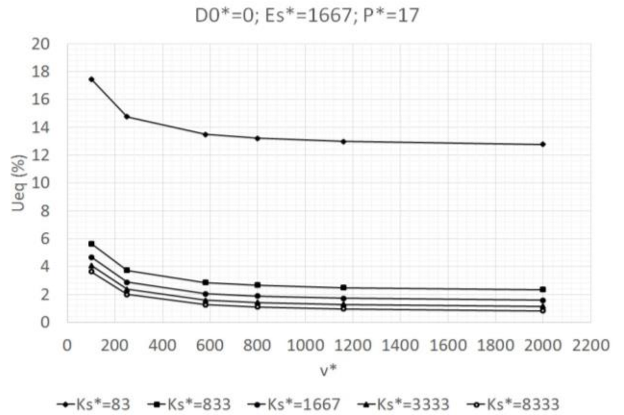

(b)

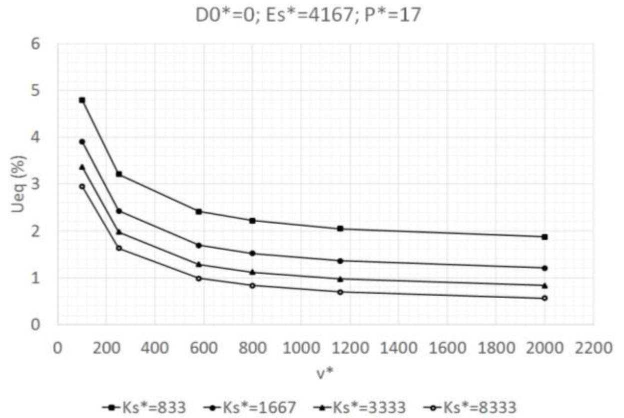

(c)

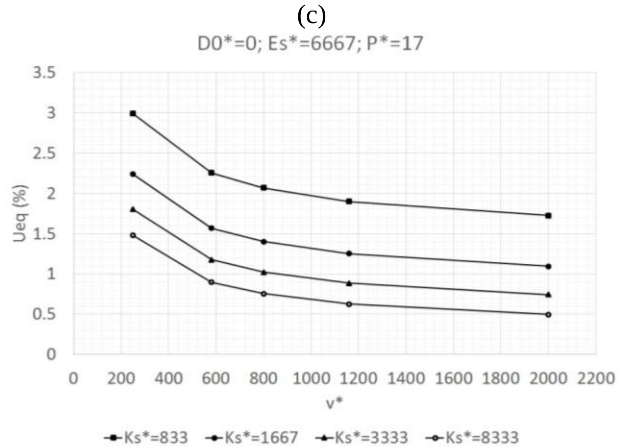

(d)

Fig. 15 Group 2: D0*=0, P*=17, Es*=80 to 6667

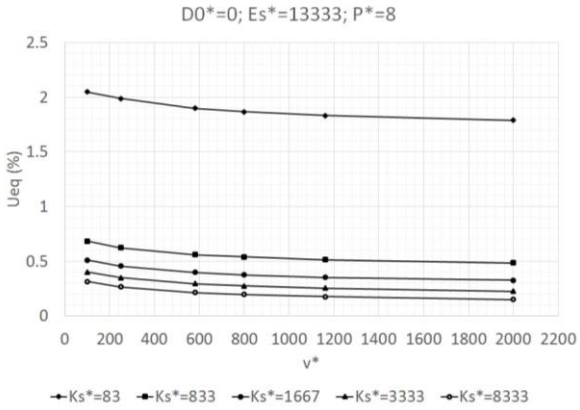

(a)

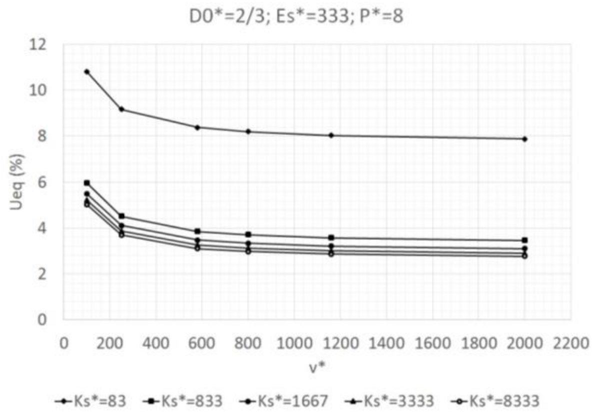

(b)

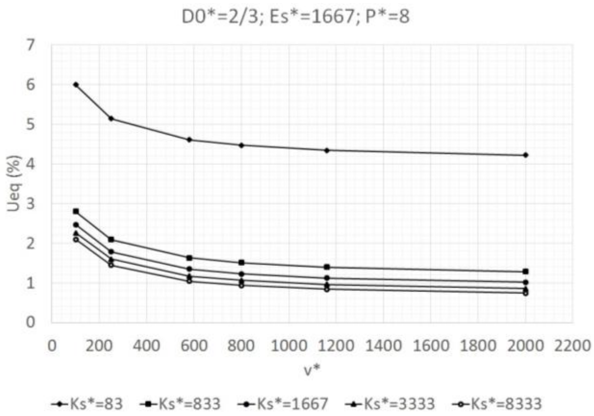

(c)

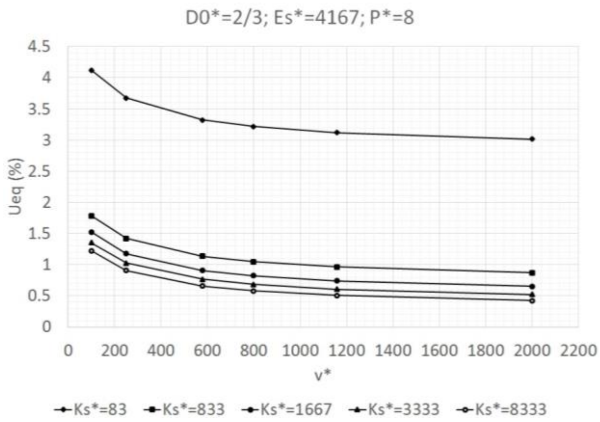

(d)

Fig. 16 Group 2: D0*=0, P*=8, Es*=13333; D0*=2/3, P*=8, Es*=333 to 4167

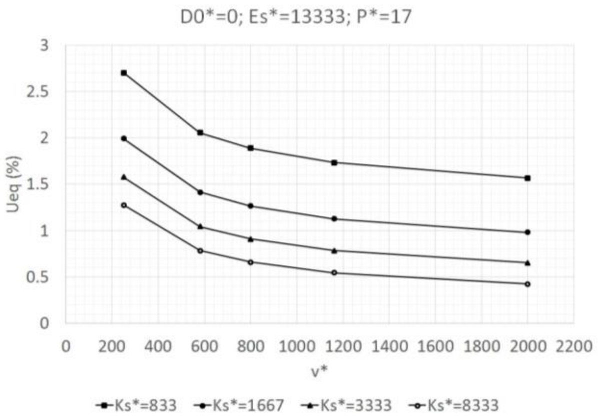

(a)

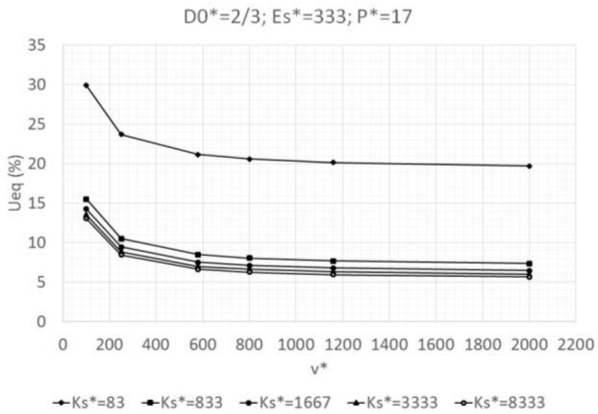

(b)

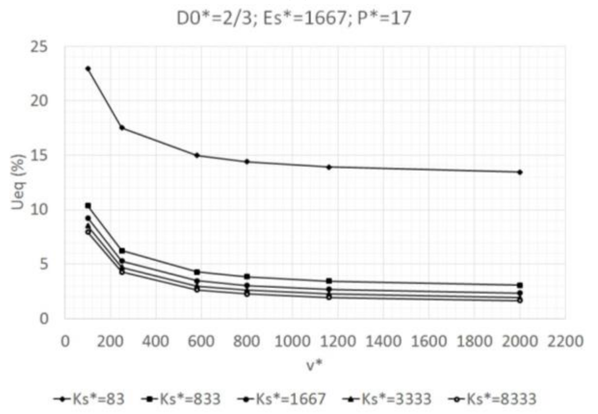

(c)

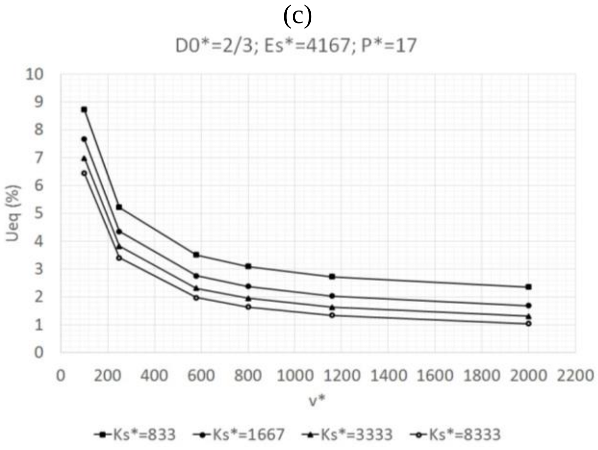

(d)

Fig. 17 Group 2: D0*=0, P*=17, Es*=13333; D0*=2/3, P*=17, Es*=333 to 4167

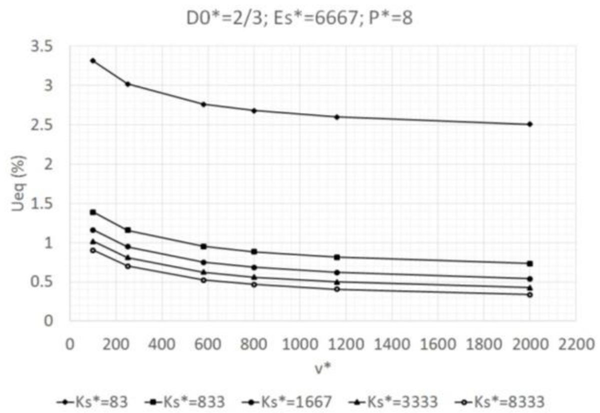

(a)

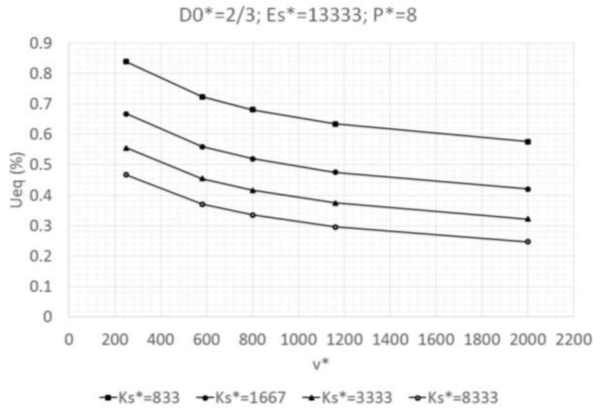

(b)

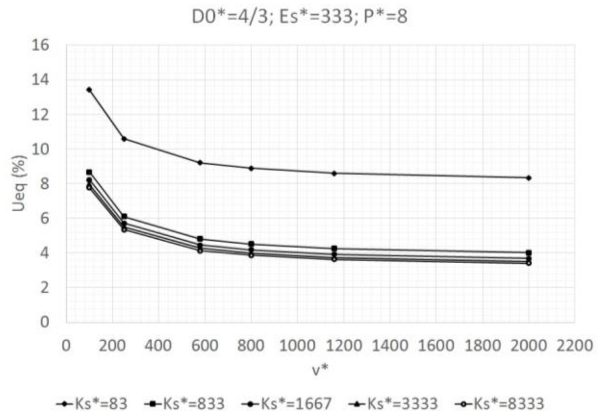

(c)

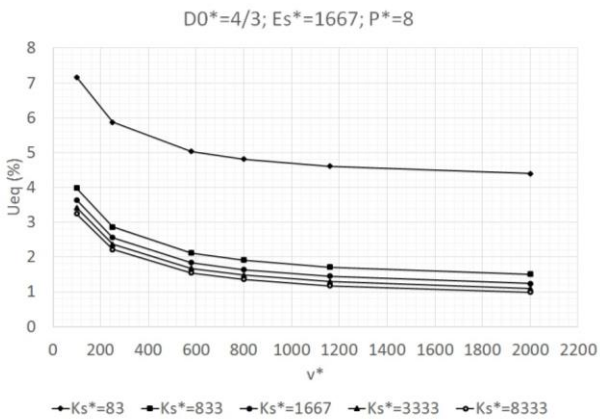

(d)

Fig. 18 Group 2: D0*=2/3, P*=8, Es*=6667 to 13333; D0*=4/3, P*=8, Es*=333 to 1667

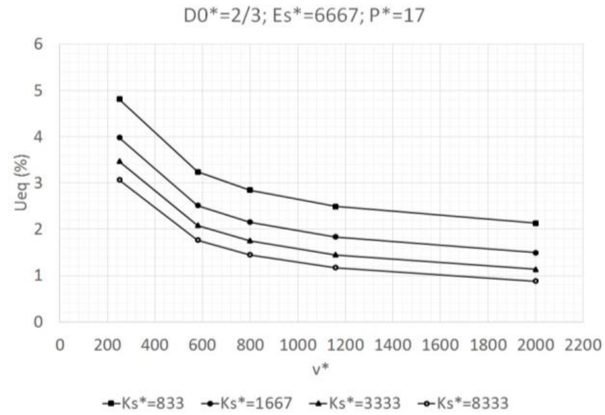

(a)

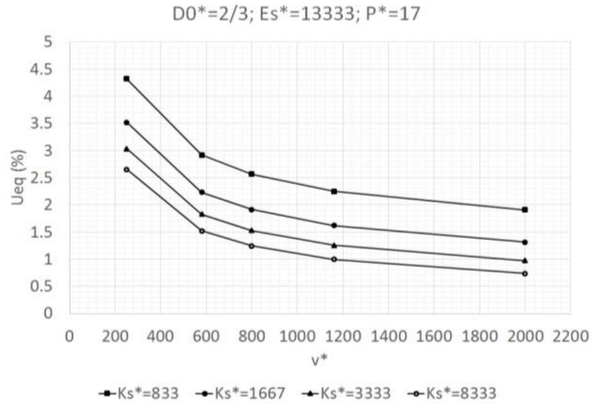

(b)

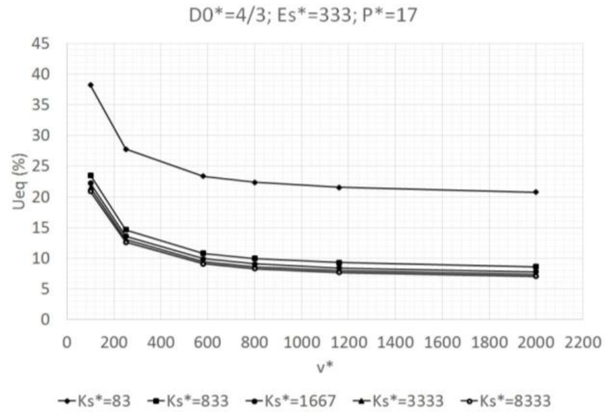

(c)

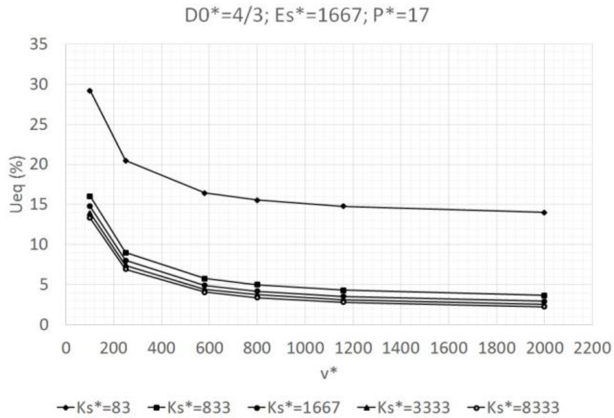

(d)

Fig. 19 Group 2: D0*=2/3, P*=17, Es*=6667 to 13333; D0*=4/3, P*=17, Es*=333 to 1667

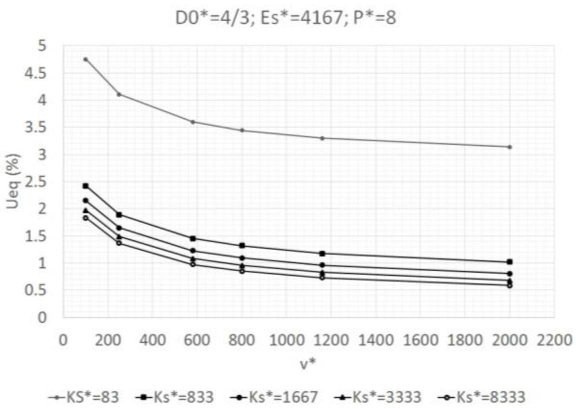

(a)

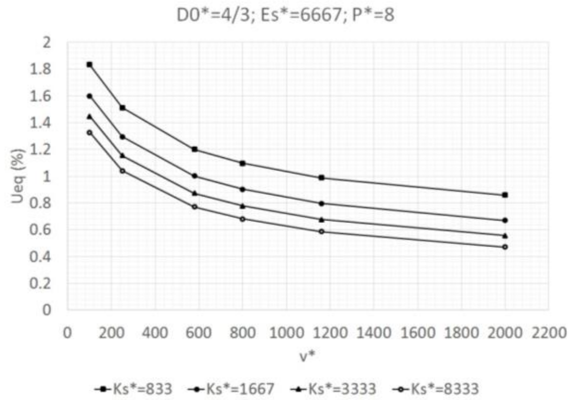

(b)

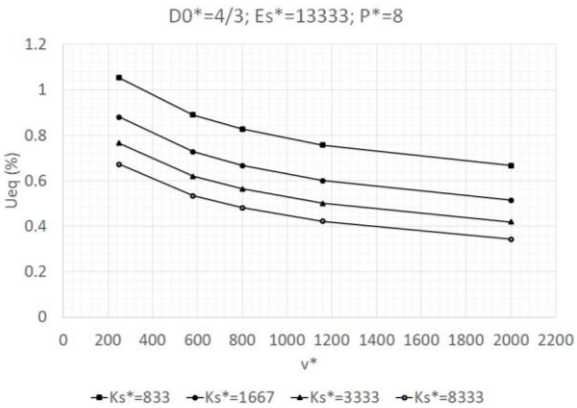

(c)

Fig. 20 Group 2 D0*=4/3, P*=8, Es*=4167 to 13333

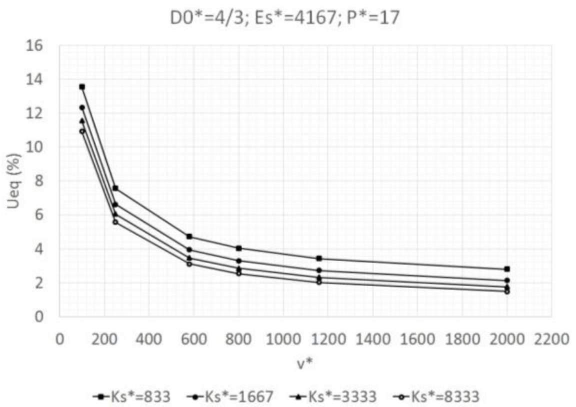

(a)

Fig. 21 Group 2 D0*=4/3, P*=17, Es*=4167 to 13333

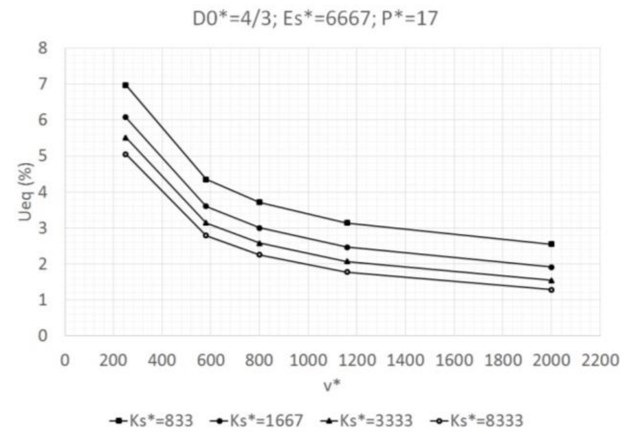

(b)

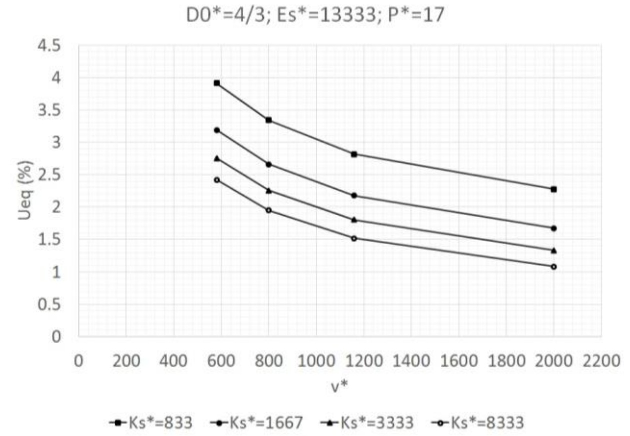

(c)

Fig. 21 Continued

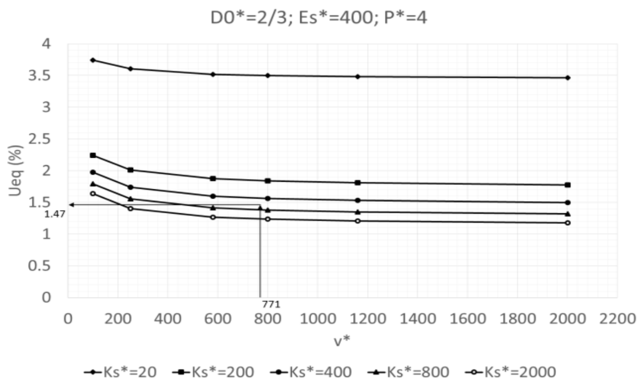

Fig. 22 Example of using the abacus

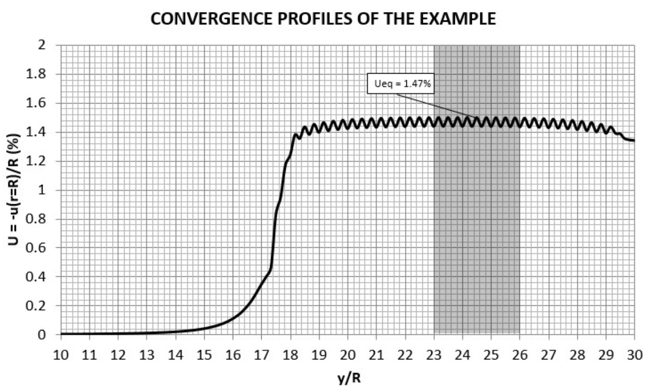

Fig. 23 Convergence profile of the example

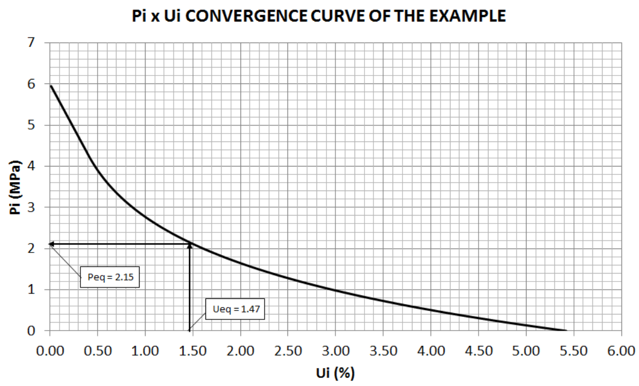

Fig. 24 Pi x Ui Convergence curve of the example

5. Example of abacus utilization

Input data: R = 4m, e = 0,1m; H=353m; γ = 17kN/m³; E_s=600MPa; ν_s=0.4; C = 1.5MPa; η = 107 MPa.s; d_0 = 2/3R; E_r = 30000MPa e V = 10m/day. Initially it is checked if the parameters d_0*, E_s*, ν_s e P* are in the scope of the abacus

$$E_s^* = \frac{E_s}{C} = \frac{600MPa}{1.5MPa} = 400 \rightarrow (OK) \tag{20}$$

$$P^* = \frac{\gamma H}{C} = \frac{(17kN/m^3)*353m}{1.5MPa} = \frac{6MPa}{1.5MPa} = 4 \rightarrow (OK) \tag{21}$$

$$\nu_s = 0.4 \rightarrow (OK) \tag{22}$$

Once these parameters are within the scope of the abacus, you can continue the calculations

$$K_s = \frac{E_r(R^2-(R-e)^2)}{(1+\upsilon_r)\left[(1-2\upsilon_r)R^2+(R-e)^2\right]} = \frac{30000(4^2-(3.9)^2)}{(1+0.3)\left[(1-2*0.3)4^2+(3.9)^2\right]} = 843.6MPa \tag{23}$$

$$K_s^* = \frac{K_s}{C} = \frac{843MPa}{1.5MPa} = 562.4 \tag{24}$$

$$V^* = \frac{V\eta}{CR} = \frac{\left(10\dfrac{m}{day}\right)*10^7\,MPa\cdot s}{1.5MPa*1m}\left(\frac{1day}{60*60*24s}\right) = 771 \tag{25}$$

With the values of d_0*, E_s*, P*, K_s* e V* go to the abacus according to Fig. 22.

The convergence profile of the example is shown in Fig. 23.

Drawing the convergence curve of the Eq. (17) we can find the pressure P_{eq} as shown in Fig. 24.

In another way, using Eq. (19)

$$P_{eq} = 6 - \frac{2}{\sqrt{3}}*1.5\left[1+\ln\left(\frac{2*0.0147*600}{3*\dfrac{2}{\sqrt{3}}*1.5}\right)\right] = 2.15MPa \tag{26}$$

6. Conclusions

In this paper, we show the results of a parametric study from finite element method involving 1716 analysis summarized in 60 abacuses. It consists of a very useful tool for preliminaries study of tunnels. We can observed the influence of the dimensionless parameters in the long time behavior of the tunnel. For example, the larger the unlined distance the greater the radial displacements. For sequential excavations (mining type) it is difficult to work with small unlined distances due to the space required to move the machines. Therefore, if it is necessary to reduce the radial deformation the use of tunnel-boring machines (TBM) is suggested. If P* is less than 2 then the use of lower speeds can be reached because in this case there is little influence on radial displacement. However, if P* is greater than 2 then, to obtain smaller displacements, higher speeds should be prioritized.

To determine the pressure at equilibrium, the convergence curve of rock mass can be calculated from Eqs. (15)-(18). However, the results obtained from this curve present a very good agreement with the results of Eq. (19).

The results of the abacuses are deduced for deep tunnels. Nevertheless, they can be used as a first approach for shallow tunnels.

References

Barla, G., Debernardi, D. and Sterpi, D. (2011), "Time-dependent modeling of tunnels in squeezing conditions", *J. Geomech.*, **12**(6), 697-710.

Benamar, I. (1996), "Etude des effets différés dans tunnels profonds", Ph.D. Dissertation, Ecole Nationale des Ponts et Chaussées, Paris, France (in French).

Bernaud, D. (1991), "Tunnels profonds dans les milieu viscoplastiques: Approaches expérimentale et numérique", Ph.D. Dissertation, Ecole Nationale des Ponts et Chaussées, Paris, France.

Bernaud, D. and Rousset, G. (1992), "La « nouvelle méthode implicite » pour l'étude du dimensionnement des tunnels", *Rev. Franç. Géotech.*, (60), 5-26 (in French).

Bernaud, D. and Rousset, G. (1993), L'essai de soutènement à convergence controlée: Résultats et modélisation, *Proceedings of the International Symposium: Hard Soils-Soft Rocks,* Athens, Greece, September.

Bernaud, D., Benamar, I. and Rousset, G. (1994), "La nouvelle methode implicite pour le calcul des tunnels dans les milieux élastoplastiques et viscoplastiques", *Rev. Franç. Géotech.*, (68), 3-19 (in French).

Boidy, E., Bouvard, A. and Pellet, F. (2002), "Back analysis of time-dependent behaviour of a test gallery in claystone", *Tunn. Undergr. Sp. Technol.*, **17**(4), 415-424.

Couto, E.C. (2011), "Um modelo tridimensional para túneis escavados em rocha reforçada por tirantes passivos", Ph.D. Dissertation, Universidade Federal do Rio Grande do Sul, Porto Alegre, Brazil (in Portuguese).

Debernardi, D. (2008), "Viscoplastic behavior and design of tunnels", Ph.D. Dissertation, Polytechnic University of Turin, Turin, Italy.

Debernardi, D. and Barla, G. (2009), "New viscoplastic model for design analysis of tunnels in squeezing conditions", *Rock Mech. Rock Eng.*, **42**(2), 259-288.

Fahimifar, A., Tehrani, F.M., Hedayat, A. and Vakilzadeh, A. (2010), "Analytical solution for the excavation of circular tunnels in a visco-elastic Burger's material under hydrostatic stress field", *Tunn. Undergr. Sp. Technol.*, **25**(4), 297-304.

Fiore, P.V., Maghous, D.B. and Campos Filho, A. (2016), "A tridimensional finite elemento approach to model a tunnel with shotcrete and precast concrete", *Ibracon Struct. Mater. J.*, **9**(3), 403-413.

Gomes, R.A.M.P. (2006), "Análise tridimensional de túneis considerando o comportamento dependente do tempo na interação maciço-suporte", Ph.D. Dissertation, São Carlos da Universidade de São Paulo, São Paulo, Brazil (in Portuguese).

Hanafy, E.A. (1981), "Simulation of tunnel excavations in squeezing ground", Ph.D. Dissertation, McMaster University, Hamilton, Canada.

Karami, M. and Fahimifar, A. (2013), *A New Time-Dependent Constitutive Model and its Application in Underground Construction*, in *RapidMiner: Data Mining Use Cases and Business Analytics Applications*, 437-440.

Khoshboresh, A.R. (2013), "A Study on deformation of tunnels excavated in fracture rocks", M.Sc. Dissertation, Université Laval, Quebec, Canada.

Machado, G.M. (2011), "Análise por elementos finitos de maciços escavados por túneis", M.Sc. Dissertation, Escola Politécnica da Universidade de São Paulo, São Paulo, Brazil (in Portuguese).

Malan, D.F. (1999), "Time-dependent behavior of deep level tabular excavations in hard rock", *Rock Mech. Rock Eng.*, **32**(2), 123-155.

Maleki, M. and Mousivand, M. (2014), "Safety evaluation of shallow tunnel based on elastoplastic-viscoplastic analysis", *Scientia Iranica Trans. A Civ. Eng.*, **21**(5), 1480.

Masin, D. (2009), "3D modeling of a NATM tunnel in high K0 clay using two different constitutive models", *J. Geotech. Geoenviron. Eng.*, **135**(9), 1326-1335.

Mroueh, H. and Shahrour, I. (2003), "A full 3-D finite element analysis of tunneling-adjacent structures interaction", *Comput. Geotech.*, **30**(3), 245-253.

Nomikos, P., Rahmannejad, R. and Sofianos, A. (2011), "Supported axisymmetric tunnels within linear viscoelastic Burgers rocks", *Rock Mech. Rock Eng.*, **44**(5), 553-564.

Pan, Y.W. and Dong, J.J. (1991a), "Time-dependent tunnel convergence-I. Formulation of the model", *J. Rock Mech. Min. Sci. Geomech. Abstr.*, **28**(6), 469-475.

Pan, Y.W. and Dong, J.J. (1991b), "Time-dependent tunnel convergence-II. Advance rate and tunnel-support interaction", *J. Rock Mech. Min. Sci. Geomech. Abstr.*, **28**(6), 477-488.

Panet,M. (1995), *Le Calcul Des Tunnels Par La Méthode Convergence-Confinement*, Presses de l'école Nationale des Ponts et Chausseés, Paris, France (in French).

Quevedo, F.P.M. (2017), "Comportamento a longo prazo de túneis profundos revestidos com concreto: Modelo em elementos finitos", M.Sc. Disseration, UFRGS, Porto Alegre, Brazil (in Portuguese).

Roatesi, S. (2010), "Analysis of the successive phases of a tunnel excavation with support mounting", *Proc. Roman. Acad. Ser. A*, **11**, 11-18.

Sahli, M., Pellet, F., Boidy, E. and Fabre, G. (2001), "Modeling of viscous behavior of rocks for deep tunnels", *Proceedings of the ISRM Regional Symposium, Eurock*, Espoo, Finland, June.

Sharifzdadeh, M., Tarifard, A. and Moridi, M.A. (2013), "Time-dependent behavior of tunnel lining in weak rock mass based on displacement back analysis method", *Tunn. Undergr. Sp. Technol.*, **38**, 348-356.

Sterpi, D. and Gioda, G. (2009), "Visco-plastic behavior around advancing tunnels in squeezing rock", *Rock Mech. Rock Eng.*, **42**(2), 319-339.

Sulem, J., Panet, M. and Guenot, A. (1987), "An analytical solution for time-dependent displacements in a circular tunnel", *J. Rock Mech. Min. Sci. Geomech. Abstr.*, **24**(3), 155-164.

Wang, H.N., Li, Y., Ni, Q., Utili, S., Jiang, M.J. and Liu, F. (2013), "Analytical solutions for the construction of deeply buried

circular tunnels with two liners in rheological rock", *Rock Mech. Rock Eng.*, **46**(6), 1481-1498.
Wang, H.N., Utili, S. and Jiang, M.J. (2014), "An analytical approach for the sequential excavation of axisymmetric lined tunnels in viscoelastic rock", *J. Rock Mech. Min. Sci.*, **68**, 85-106.

CC